

Depletion of CD4⁺ T cells abrogates post-peak decline of viremia in SIV-infected rhesus macaques

Alexandra M. Ortiz,^{1,2,3} Nichole R. Klatt,⁴ Bing Li,¹ Yanjie Yi,^{2,5} Brian Tabb,⁶ Xing Pei Hao,⁶ Lawrence Sternberg,⁶ Benton Lawson,¹ Paul M. Carnathan,^{1,3} Elizabeth M. Cramer,^{2,3} Jessica C. Engram,³ Dawn M. Little,⁷ Elena Ryzhova,⁸ Francisco Gonzalez-Scarano,⁸ Mirko Paiardini,^{1,3} Aftab A. Ansari,⁷ Sarah Ratcliffe,⁹ James G. Else,¹ Jason M. Brenchley,⁴ Ronald G. Collman,^{2,5} Jacob D. Estes,⁶ Cynthia A. Derdeyn,¹ and Guido Silvestri^{1,3,7}

¹Yerkes National Primate Research Center and Emory Vaccine Center, Emory University, Atlanta, Georgia, USA. ²Department of Microbiology and

³Department of Pathology and Laboratory Medicine, University of Pennsylvania School of Medicine, Philadelphia, Pennsylvania, USA.

⁴Laboratory of Molecular Microbiology, NIH, Bethesda, Maryland, USA. ⁵Department of Medicine, University of Pennsylvania School of Medicine, Philadelphia, Pennsylvania, USA. ⁶AIDS and Cancer Virus Program, SAIC-Frederick, National Cancer Institute, NIH, Frederick, Maryland, USA.

⁷Department of Pathology and Laboratory Medicine, Emory University, Atlanta, Georgia, USA. ⁸Department of Neurology and

⁹Department of Biostatistics, University of Pennsylvania School of Medicine, Philadelphia, Pennsylvania, USA.

CD4⁺ T cells play a central role in the immunopathogenesis of HIV/AIDS, and their depletion during chronic HIV infection is a hallmark of disease progression. However, the relative contribution of CD4⁺ T cells as mediators of antiviral immune responses and targets for virus replication is still unclear. Here, we have generated data in SIV-infected rhesus macaques (RMs) that suggest that CD4⁺ T cells are essential in establishing control of virus replication during acute infection. To directly assess the role of CD4⁺ T cells during primary SIV infection, we in vivo depleted these cells from RMs prior to infecting the primates with a pathogenic strain of SIV. Compared with undepleted animals, CD4⁺ lymphocyte-depleted RMs showed a similar peak of viremia, but did not manifest any post-peak decline of virus replication despite CD8⁺ T cell- and B cell-mediated SIV-specific immune responses comparable to those observed in control animals. Interestingly, depleted animals displayed rapid disease progression, which was associated with increased virus replication in non-T cells as well as the emergence of CD4-independent SIV-envelopes. Our results suggest that the antiviral CD4⁺ T cell response may play an important role in limiting SIV replication, which has implications for the design of HIV vaccines.

Introduction

The interaction between HIV and the host immune system is complex, with both suppression of virus replication by certain immune mediators (e.g., CD8⁺ T lymphocytes, neutralizing Abs, and Ab-dependent cellular cytotoxicity [ADCC]; reviewed in ref. 1) and facilitation of virus transmission and/or replication by others (e.g., activated CD4⁺CCR5⁺ T cells and DCs; reviewed in refs. 2, 3). This complexity is one of the reasons why an effective AIDS vaccine has yet to be designed. In particular, the interaction between CD4⁺ T cells and HIV may result in contrasting effects with respect to virus replication. On one hand, HIV-specific CD4⁺ T cells provide help for both HIV-specific CD8⁺ T cells and B cells, thus resulting in strong cytotoxic T lymphocyte (CTL) activity and production of HIV-specific Abs (reviewed in refs. 4, 5). On the other hand, activated CD4⁺ T cells are key targets for HIV replication, and their presence in mucosal sites may favor virus transmission and/or replication (2, 6–8).

The host antiviral immune response during HIV infection has been studied using the in vivo experimental model of pathogenic SIV_{mac} infection of rhesus macaques (RMs), which results in a disease similar to HIV infection in humans. By performing in vivo depletion of specific cell populations with mAbs as well as adoptive transfer of SIV-specific Abs, it has been established that both CD8⁺ T lymphocytes and neutralizing Abs suppress virus replication in

SIV-infected RMs (9–15). A potential antiviral role of CD4⁺ T helper cells in determining the level of virus replication was suggested by an experiment in which RMs were subjected to a costimulatory blockade with CTLA-1g and anti-CD40L Abs at the time of primary SIV infection, resulting in abrogation of the post-peak decline of viremia (16). However, in that study, both T cell- and B cell-mediated SIV-specific immune responses were significantly disrupted, thus precluding a direct assessment of the role of CD4⁺ T cells. To directly measure the role of CD4⁺ T cells in determining the level of peak viremia and the magnitude of the post-peak decline during primary SIV infection, we depleted CD4⁺ lymphocytes in vivo in 5 Indian RMs by administering the humanized anti-CD4 mAb Cdr-OKT4A-huIgG1, and included 4 age- and gender-matched animals as undepleted controls. In this study, we selected a treatment protocol that depletes the vast majority of circulating CD4⁺ T cells, as well as those resident in LNs and BM, but has only a marginal effect on the level of mucosal CD4⁺ T cells. The rationales for this choice were (a) to preserve the overall dynamics of early SIV replication and dissemination that mainly occur in mucosal tissues during the acute phase of infection (17–19), (b) to selectively abrogate the function of CD4⁺ T helper cells in inductive sites, and (c) to reduce the availability of CD4⁺ target cells in the post-peak phase of primary viremia (i.e., after virus-mediated depletion of mucosal CD4⁺ T cells). We also reasoned that this treatment would not change the effect of antiviral CD8⁺ T cell responses, based on the current paradigm that priming of virus-specific CTL responses is independent of

Conflict of interest: The authors have declared that no conflict of interest exists.

Citation for this article: *J Clin Invest.* 2011;121(11):4433–4445. doi:10.1172/JCI46023.

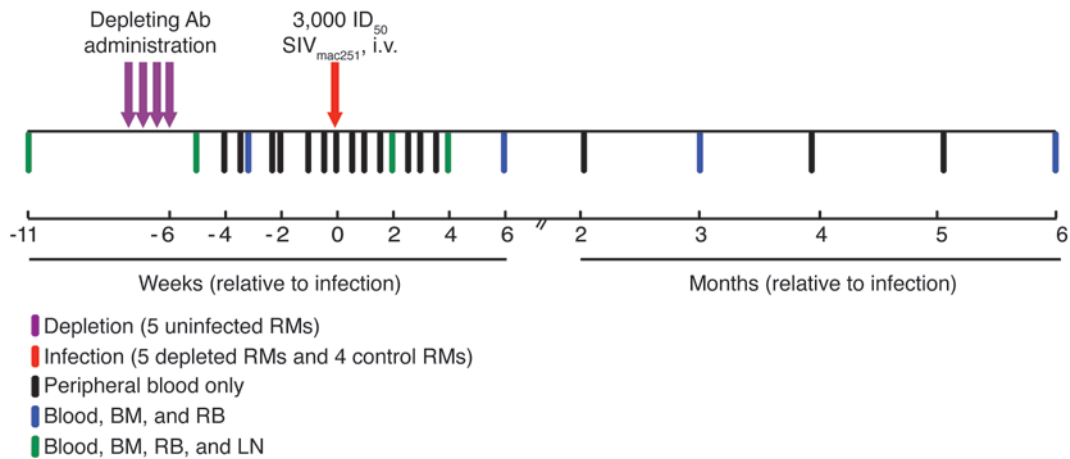


Figure 1

Experimental design of CD4⁺ lymphocyte depletion and SIV infection. 5 RMs were treated with the CD4⁺ lymphocyte–depleting Ab Cdr-OKT4A-huIgG1 prior to SIV infection, while 4 control animals were infected without any prior treatment. Samples of peripheral blood, BM, RB, and LN were collected at various time points before and after SIV infection.

CD4⁺ T cell help (20–22). Similarly, we reasoned that this treatment would not influence the antiviral effect of SIV-specific neutralizing Abs, as they do not become detectable until after the acute stage of SIV_{mac} infection (23–25). Finally, we proposed that by inoculating RMs with SIV after a 6-week washout period from the last infusion of Cdr-OKT4A-huIgG1, we would avoid the potential confounding factor of direct antiviral activity of this anti-CD4 Ab (26).

We found that CD4⁺ lymphocyte–depleted, SIV-infected RMs reached a peak level of virus replication very similar to that observed in undepleted controls. However, CD4⁺ lymphocyte–depleted RMs did not manifest a post-peak decline of virus replication despite CD8⁺ T cell- and B cell-mediated SIV-specific immune responses that were comparable to those of undepleted animals. As expected, this inability to control virus replication was associated with rapid disease progression. Since there was no evidence of a substantial increase in CD4⁺ target cells (i.e., total or memory CD4⁺ T cells expressing Ki67 and/or CCR5) in the CD4⁺ lymphocyte–depleted RMs, our findings support the possibility of a direct antiviral effect of CD4⁺ T cells during primary SIV infection.

Results

Experimental design. To investigate the in vivo role of CD4⁺ T cells during primary SIV_{mac} infection of RMs as either mediators of antiviral immune responses or targets for virus replication, we depleted CD4⁺ lymphocytes from 5 RMs using the humanized mAb Cdr-OKT4A-huIgG1, administered i.v. 4 times over 12 days at a dose of 10 mg/kg. The study also included 4 undepleted animals as controls. All RMs were infected i.v. with 3,000 tissue culture ID₅₀ (TCID₅₀) of SIV_{mac251} at day 45 after the last Cdr-OKT4A-huIgG1 administration, and tissues (BM and LN as well as rectal mucosa via rectal biopsy, referred to herein as RB) and peripheral blood were sampled at multiple time points throughout the study (Figure 1). This 45-day washout period prior to SIV infection was considered sufficient to remove the potential confounder of a direct antiviral effect mediated by Cdr-OKT4A-huIgG1.

Anti-CD4 Ab induces major CD4⁺ T cell depletion in blood, LNs, and BM. The efficacy of the anti-CD4 Ab in depleting CD4⁺ T cells in vivo was assessed in each examined site by multiparametric flow cytometry.

As expected, treated RMs exhibited a major decrease (approximately 90%–95% relative to baseline) in both the percentage and absolute number of peripheral blood CD4⁺ T cells that persisted until the time of infection (Figure 2, A and B). Of note, one of the treated RMs, animal RUv6, exhibited less dramatic CD4⁺ T cell depletion; therefore, we presented results from this animal separately from the others. Prior to treatment with the anti-CD4 Ab, RMs in the treatment group showed 55.8% ± 14.0% CD3⁺CD4⁺ T cells and an absolute count of 765.6 ± 362.9 CD4⁺ T cells/μl in peripheral blood (Figure 2B). Similarly, control animals exhibited 60.9% ± 10.2% CD3⁺CD4⁺ T cells and an absolute count of 876.4 ± 394.6 CD4⁺ T cells/μl in peripheral blood. At the nadir of depletion, the level of circulating CD4⁺ T cells was 3.6% ± 0.6% of CD3⁺ T cells, with an absolute count of 5.0 ± 4.3 CD4⁺ T cells/μl. By the time of SIV infection, the level of circulating CD4⁺ T cells was 15.3% ± 5.5% of CD3⁺ T cells, with an absolute count of 65.4 ± 44.8 CD4⁺ T cells/μl, representing an average decrease of 91.4% ± 3.0% of the absolute number of CD4⁺ T cells compared with baseline. The depleting treatment similarly affected all of the main CD4⁺ T cell subsets, including naive, central memory, effector memory, and regulatory cells (data not shown). In contrast, in untreated RMs, circulating CD4⁺ T cells at the time of experimental SIV infection represented 57.8% ± 1.2% of CD3⁺ T cells, an absolute count of 659.8 ± 597.8 CD4⁺ T cells/μl (*P* = NS vs. baseline; Figure 2B). We next measured the relative percentage of CD3⁺CD4⁺ T cells within the BM, LN, and RB. As shown in Figure 2C, treatment with anti-CD4 Ab induced a substantial depletion of CD4⁺ T cells in the BM and LNs (mean decline of 90.1% ± 1.9% and 75.5% ± 18.0%, respectively, relative to baseline), but not in the RB, in which depleted RMs exhibited levels of CD4⁺ T cells similar to those of undepleted controls (54.3% ± 24.7% and 31.1% ± 6.7% of CD3⁺ T cells, respectively; *P* = NS). Importantly, the effect of Cdr-OKT4A-huIgG1 was highly specific for CD4⁺ T cells, as other subsets of circulating or tissue-based mononuclear cells (i.e., monocytes, B cells, NK cells, and CD8⁺ T cells) were not affected by this treatment (Supplemental Figure 1; supplemental material available online with this article; doi:10.1172/JCI46023DS1). Similarly, no changes in the levels of circulating plasmacytoid and myeloid DCs were observed

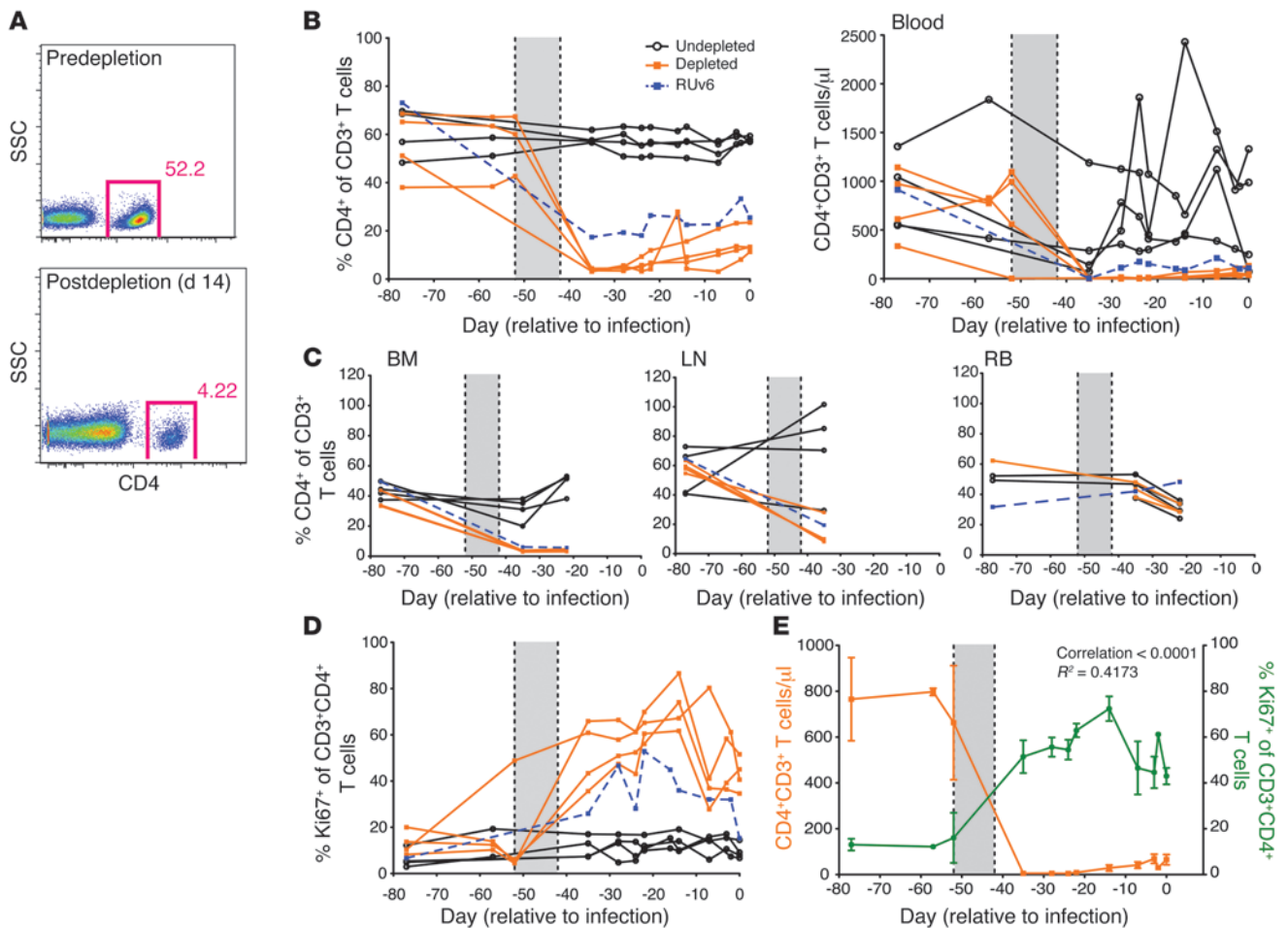


Figure 2

Anti-CD4 Ab induces major CD4⁺ T cell loss in blood, LN, and BM, followed by residual CD4⁺ T cell proliferation. (A) Representative flow cytometry plots of percent circulating CD4⁺ T cells (relative to total CD3⁺ T cells) before and after Cdr-OKT4A-hulgG1 treatment. (B) Longitudinal assessment of percent and absolute number per μl of peripheral blood CD4⁺ T cells before and after Cdr-OKT4A-hulgG1 treatment. CD4⁺ T cell dynamics were significantly different between CD4⁺ lymphocyte-depleted RMs and controls from baseline to the time of infection ($P < 0.001$, linear mixed-effects model). (C) Longitudinal assessment of percent CD4⁺ T cells in the BM, LN, and RB. Percent CD3⁺CD4⁺ T cells was significantly lower in the BM ($P = 0.0011$) and LN ($P = 0.0378$) of CD4⁺ lymphocyte-depleted RMs (Student's t test with Welch correction). Some baseline time points were unavailable in RB due to technical error ($n = 4$). (D) Longitudinal assessment of percent CD4⁺Ki67⁺ T cells in peripheral blood, significantly higher at the time of infection in CD4⁺ lymphocyte-depleted RMs ($P = 0.0062$, Student's t test with Welch correction). (E) Correlation between peripheral CD4⁺ T cell absolute count (orange) and percent CD4⁺Ki67⁺ T cells (green) in CD4⁺ lymphocyte-depleted animals ($P < 0.0001$, $R^2 = 0.4173$). Shaded area represents time of CD4⁺ lymphocyte-depleting treatment.

after treatment with the anti-CD4 Ab (data not shown). Of note, the levels of circulating anti-CD4 Ab at the last time point prior to infection (i.e., day 45 after depletion) were assessed as serum CD4-binding activity by incubating serial dilutions of serum with the CD4-expressing cell line HUT78 and measuring binding activity by flow cytometry. This analysis revealed that, at day 45 after depletion (i.e., time of SIV infection), the binding of CD4 by the sera of depleted animals was slightly increased compared with that of undepleted animals (average MFI increase of 38.7%, as opposed to 327% of the sera collected immediately after infusion, data not shown), with the exception of animal RZj5, which showed CD4 binding levels similar to the positive controls.

Anti-CD4 Ab-mediated CD4⁺ lymphocyte depletion is followed by increased proliferation of residual CD4⁺ T cells. In vivo depletion of CD4⁺ lymphocytes in nonhuman primates is followed by homeostatic proliferation

of residual CD4⁺ T cells, which involves preferentially non-naive cells (27, 28). To confirm this phenomenon in our group of CD4⁺ lymphocyte-depleted RMs, we longitudinally measured the expression of the proliferation marker Ki67 on CD4⁺ T cells by flow cytometry in blood and tissues (LN, BM, and RB). As shown in Figure 2, D and E, after CD4⁺ lymphocyte depletion, residual peripheral blood CD4⁺ T cells exhibited a marked increase in Ki67 expression, with a significant inverse correlation between absolute number of CD4⁺ T cells and percent circulating CD4⁺ T cells expressing Ki67 ($R^2 = 0.4173$; $P < 0.0001$). Of note, depletion of CD4⁺ T cells did not induce an increase in the level of proliferating CD8⁺ T cells (data not shown). This relationship between absolute CD4⁺ T cell count and fraction of CD4⁺Ki67⁺ cells was absent in undepleted control animals (data not shown). The difference in percent CD4⁺Ki67⁺ T cells between depleted RMs and undepleted controls remained significant at the

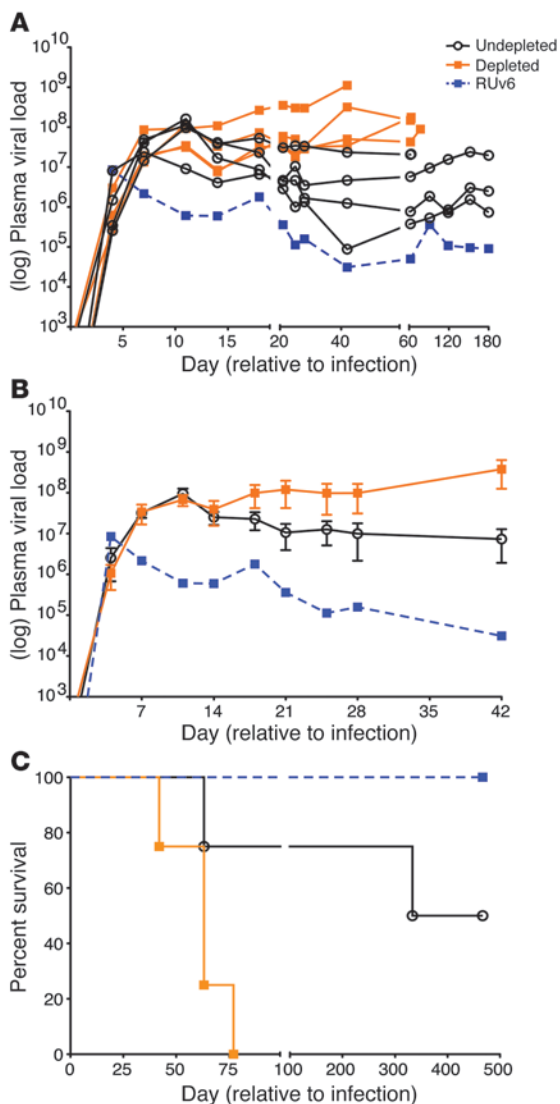


Figure 3

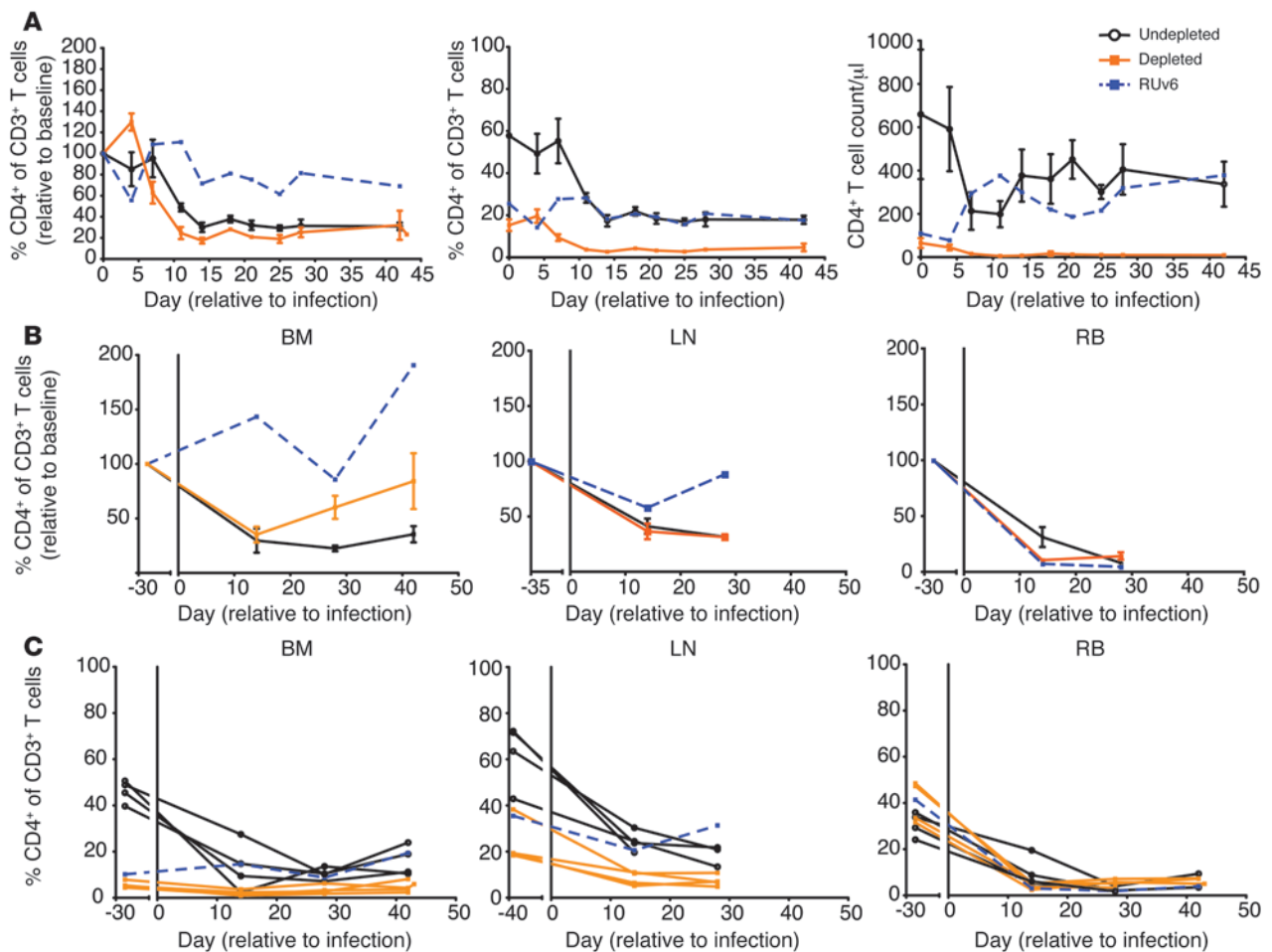
CD4⁺ lymphocyte depletion is associated with the absence of post-peak decline of viremia and with accelerated disease progression. Longitudinal assessment of plasma viremia expressed as log plasma viral load for individual animals (A) and mean ± SEM of the log plasma viral load (B) in CD4⁺ lymphocyte-depleted and control RMs. Setpoint viral loads (days 18–42 p.i.) were significantly higher in treated animals (P = 0.044, log plasma viral load, linear mixed effects model). (C) Survival curves for CD4⁺ lymphocyte-depleted and control RMs (P = 0.0414, hazard ratio 8.317, Kaplan-Meier estimate through day 467).

time of infection (P = 0.006, Student's *t* test with Welch correction for unequal variances). As expected based on the finding that our treatment depleted CD4⁺ T cells in LN and BM, but not in RB, we observed an increase in the fraction of CD4⁺Ki67⁺ T cells in the LN and BM of the depleted RMs, but not in RB (data not shown). In all, these data confirmed that experimental CD4⁺ lymphocyte depletion is associated with a lineage- and tissue-specific increased proliferation of the residual CD4⁺ T cells.

SIV infection of CD4⁺ T lymphocyte-depleted RMs is characterized by absence of post-peak viral decline and rapid progression to AIDS. After completion of the CD4⁺ lymphocyte-depleting protocol, all animals were infected with 3,000 TCID₅₀ SIV_{mac251} (day 0). We then examined the kinetics of SIV plasma viremia. As shown in Figure 3, A and B, both groups of animals experienced a rapid, exponential increase in virus replication that reached a maximum level at approximately day 11 post infection (p.i.; control, 9.5 × 10⁷ ± 6.3 × 10⁷ copies/ml; CD4⁺ lymphocyte-depleted, 6.8 × 10⁷ ± 4.1 × 10⁷; P = NS). Importantly, whereas the control, undepleted SIV-infected RMs showed a discernible post-peak decline of viremia (i.e., 1–2 logs on average), the 4 fully CD4⁺ lymphocyte-depleted SIV-

infected RMs did not display a clear post-peak decline of viremia and maintained a mean setpoint viral load greater than 1 log higher than that of control animals. This difference was statistically significant between days 14 and 42 p.i. (P = 0.001, linear mixed-effects model). Interestingly, RUv6, which had the least effective CD4⁺ lymphocyte depletion, exhibited the lowest peak and sharpest post-peak decline of viremia of all SIV-infected RMs. The more benign course of infection (i.e., lower viral load and increased survival) observed in RUv6 is unlikely to be caused by persistence of depleting Ab, since this animal showed the lowest levels of circulating anti-CD4 Ab at the last time point prior to experimental SIV infection (data not shown). Of note, the higher setpoint viremia observed in CD4⁺ lymphocyte-depleted SIV-infected RMs was associated with faster disease progression, with all 4 fully depleted animals succumbing to AIDS within 90 days of infection (Figure 3C; median survival, depleted RMs, 63 days p.i.; controls, about 400 days p.i.). This trend was considered statistically significant (P = 0.0414, hazard ratio 8.317, Kaplan-Meier estimates); however, this significance was lost when RUv6 was included in the depleted group (P = 0.2393, hazard ratio 2.914, Kaplan-Meier estimates).

SIV infection induces systemic CD4⁺ T cell loss in both CD4⁺ lymphocyte-depleted and undepleted RMs. We next assessed the effect of SIV infection on the dynamics of CD4⁺ T cells in treated and untreated RMs. Since our experimental model resulted in homeostatic proliferation of residual CD4⁺ T cells in depleted animals prior to infection, we first assessed the impact of this proliferation on the CD4⁺ T cell dynamics that typically follow SIV infection. At day 14 p.i., CD4⁺ lymphocyte-depleted RMs exhibited a mean of 2.7% ± 1.1% CD3⁺CD4⁺ T cells, with an absolute count of 7.0 ± 6.3 CD4⁺ T cells/μl, whereas control animals exhibited a mean of 17.4% ± 5.4% CD3⁺CD4⁺ T cells, with an absolute count of 377.0 ± 240.7 CD4⁺ T cells/μl (Figure 4A). Thus, the SIV-induced CD4⁺ T cell decline relative to the preinfection baseline was comparable in the 2 groups of RMs (depleted, 82.6% ± 5.4% decline; control, 70.0% ± 8.9% decline), despite the much lower CD4⁺ T cell counts observed in CD4⁺ lymphocyte-depleted animals at the time of infection. We next examined the dynamics of CD4⁺ T cells after SIV infection in the LN, BM, and RB. As shown in Figure 4, B and C, the loss of CD4⁺ T cells at day 14 p.i. in the LN was similar in control and depleted animals (declines of 58.7% ± 13.6% and 63.4% ± 14.1%, respectively). In the BM, the loss of CD4⁺ T cells at day 14 p.i. was also comparable in CD4⁺ lymphocyte-depleted and control RMs (32.7% ± 18.1% and 32.1 ± 19.8% declines, respectively), even though the levels of BM-based CD3⁺CD4⁺ T cells were higher in control RMs (13.5% ± 5.3%) than CD4⁺ lymphocyte-depleted animals (2.1% ± 0.6%). Interestingly, by day 42 p.i., the CD4⁺ lymphocyte-depleted RMs exhibited a recovery of BM-based CD4⁺ T cells to preinfection (but not pre-treatment) levels, consistent with the previously described role of the BM as a preferential anatomic site for homeostatic prolifera-

**Figure 4**

SIV infection induces systemic CD4⁺ T cell loss in both groups of CD4⁺ lymphocyte-depleted and undepleted RMs. Longitudinal assessment of CD4⁺ T cell levels after SIV infection. (A) Circulating CD4⁺ T cells, shown as percent relative to baseline (pre-SIV infection), percent of CD3⁺ T cells, and absolute CD4⁺ T cell count per μ l, in CD4⁺ lymphocyte-depleted and control RMs and RUv6. (B) Longitudinal assessment of CD4⁺ T cells (measured as percent of baseline) in the BM, LN, and RB. (C) Longitudinal assessment of CD4⁺ T cells (measured as percent of CD3⁺ T cells).

tion of CD4⁺ T cells in nonhuman primates (29). Within RBs, in which the preinfection levels of CD4⁺ T cells were similar between depleted and control RMs, SIV infection induced a similarly dramatic loss of CD4⁺ T cells in the 2 groups by day 28 p.i. (decline of $94.7\% \pm 1.6\%$ and $97.5\% \pm 1.0\%$ in depleted and control animals, respectively). Taken together, these data indicate that SIV infection had a similar effect on depleting circulating and tissue CD4⁺ T cells in CD4⁺ lymphocyte-depleted and control RMs.

CD4⁺ lymphocyte-depleted SIV-infected RMs do not show a substantial increase in activated and/or CCR5⁺CD4⁺ T cells that may serve as preferential targets for virus infection. The absence of post-peak decline of viremia in CD4⁺ lymphocyte-depleted SIV-infected RMs is consistent with 2 hypotheses: (a) defective antiviral immune responses, and (b) increased availability of target cells. While CD4⁺ lymphocyte-depleted RMs showed lower levels of total CD4⁺ T cells both at the time of SIV inoculation and throughout the acute phase of infection, we considered the possibility that the depletion-induced homeostatic proliferation of CD4⁺ T cells may have led to an absolute increase in activated (i.e., Ki67⁺) and/or CCR5⁺CD4⁺ T cells that may have acted as preferential targets for SIV infection. To address this question,

we measured the absolute levels (cells/ μ l blood for circulating CD4⁺ T cells, percentage of CD3⁺ T cells for LN- and RB-based CD4⁺ T cells) of CD4⁺Ki67⁺ T cells, CD4⁺CCR5⁺ T cells, CD4⁺Ki67⁺CCR5⁺ T cells, memory (i.e., CD95⁺) CD4⁺Ki67⁺ T cells, memory CD4⁺CCR5⁺ T cells, and memory CD4⁺Ki67⁺CCR5⁺ T cells in CD4⁺ lymphocyte-depleted and control RMs. As summarized in Table 1, none of these populations of potential preferential targets for SIV infection was increased in the CD4⁺ lymphocyte-depleted RMs at day 14 p.i. compared with control animals, and in depleted animals, only the percentage of activated/CCR5⁺CD4⁺ T cells in the RB was increased at day 28 p.i. It should be noted, however, that by day 28 p.i., the fraction of residual CD4⁺ T cells in the RB was very low in both CD4⁺ lymphocyte-depleted and control RMs (Figure 4C). Overall, these data do not support the possibility that the lack of post-peak decline of SIV viremia in depleted RMs is caused by increased numbers of CD4⁺ target cells.

CD4⁺ lymphocyte-depleted SIV-infected RMs do not show increased infection of naive CD4⁺ T cells or monocytes. We next investigated whether CD4⁺ lymphocyte depletion was associated with preferential targeting of circulating non-CD4⁺ T cells, such as monocytes, or by



Table 1

CD4⁺ lymphocyte-depleted SIV-infected RMs do not show a substantial increase in activated and/or CCR5⁺CD4⁺ T cells that may serve as preferential targets for virus infection

T cell subset	Day 14 p.i.		Day 28 p.i.		P
	Undepleted	Depleted	Undepleted	Depleted	
PBMC population (cells/μl)					
CCR5 ⁺ CD4 ⁺	6.3 \pm 7.0	0.3 \pm 0.2	6.0 \pm 5.8	3.3 \pm 6.5	NS
Ki67 ⁺ CD4 ⁺	70.8 \pm 52.3	2.7 \pm 2.4	72.5 \pm 45.6	32.3 \pm 59.4	NS
CCR5 ⁺ Ki67 ⁺ CD4 ⁺	4.3 \pm 4.5	0.2 \pm 0.1	5.2 \pm 5.1	2.9 \pm 5.7	NS
CCR5 ⁺ CD4 ⁺ memory	4.9 \pm 5.0	0.2 \pm 0.2	5.1 \pm 4.9	2.8 \pm 5.4	NS
Ki67 ⁺ CD4 ⁺ memory	48.3 \pm 36.3	2.5 \pm 2.3	55.0 \pm 33.6	23.7 \pm 42.6	NS
CCR5 ⁺ Ki67 ⁺ CD4 ⁺ memory	3.5 \pm 3.4	0.1 \pm 0.1	4.6 \pm 4.5	2.5 \pm 4.9	NS
LN (% of CD3⁺ T cells)					
CCR5 ⁺ CD4 ⁺	2.6 \pm 1.0	2.2 \pm 1.0	2.0 \pm 0.4	1.0 \pm 1.0	NS
Ki67 ⁺ CD4 ⁺	5.2 \pm 1.2	3.1 \pm 0.9	4.5 \pm 1.3	2.2 \pm 1.5	NS
CCR5 ⁺ Ki67 ⁺ CD4 ⁺	2.0 \pm 0.6	1.9 \pm 0.8	1.5 \pm 0.4	0.8 \pm 1.0	NS
CCR5 ⁺ CD4 ⁺ memory	2.6 \pm 1.2	2.0 \pm 0.8	1.7 \pm 0.4	1.0 \pm 0.9	NS
Ki67 ⁺ CD4 ⁺ memory	4.5 \pm 1.1	2.9 \pm 0.9	3.8 \pm 1.2	2.1 \pm 1.5	NS
CCR5 ⁺ Ki67 ⁺ CD4 ⁺ memory	1.9 \pm 0.7	1.8 \pm 0.7	1.4 \pm 0.4	0.8 \pm 0.9	NS
RB (% of CD3⁺ T cells)					
CCR5 ⁺ CD4 ⁺	8.4 \pm 5.8	3.7 \pm 1.5	1.6 \pm 0.9	3.7 \pm 1.7	0.0368
Ki67 ⁺ CD4 ⁺	9.1 \pm 6.7	3.7 \pm 1.4	1.9 \pm 0.8	4.4 \pm 1.3	0.0082
CCR5 ⁺ Ki67 ⁺	8.4 \pm 5.8	3.6 \pm 1.4	1.5 \pm 0.8	3.4 \pm 1.6	0.0415
CCR5 ⁺ CD4 ⁺ memory	8.2 \pm 5.5	3.5 \pm 1.4	1.5 \pm 0.8	3.6 \pm 1.6	0.0295
Ki67 ⁺ CD4 ⁺ memory	8.7 \pm 6.2	3.5 \pm 1.4	1.8 \pm 0.7	4.1 \pm 1.1	0.0061
CCR5 ⁺ Ki67 ⁺ CD4 ⁺ memory	8.1 \pm 5.5	3.4 \pm 1.4	1.5 \pm 0.7	3.4 \pm 1.5	0.0335

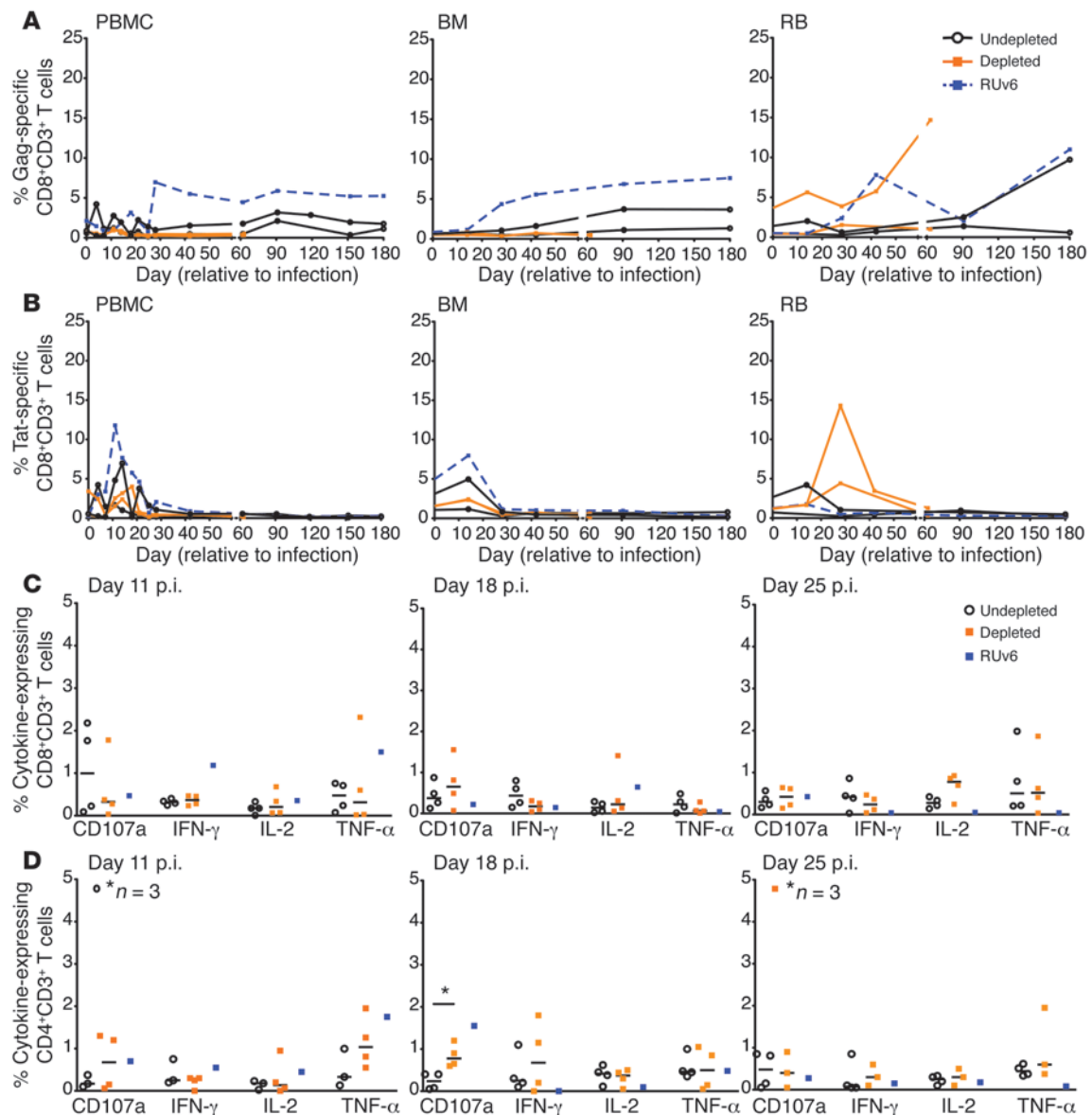
Average levels of total and memory CD4⁺ T cells expressing CCR5 and/or Ki67 (i.e., potential target cells in the blood [PBMCs], LN, and RB) at days 14 and 28 p.i. Data shown as cells/ μ l (\pm SD) for PBMCs and as percent CD3⁺ T cells for LN and BM.

an altered pattern of infected CD4⁺ T cell subsets. To this end, we measured the levels of cell-associated SIV-DNA in sorted cell populations including monocytes, naive CD4⁺ T cells (CD28⁺CD95⁻), central memory CD4⁺ T cells (CD28⁺/-CD95^{+/lo}CCR7), and effector memory CD4⁺ T cells (CD28⁻/-CD95^{+/lo}CCR7⁻). As shown in Supplemental Figure 2A, we did not observe any significant difference between CD4⁺ lymphocyte-depleted and control SIV-infected RMs in percent infected monocytes or naive CD4⁺ T cells at days 14 or 42 p.i. Similarly, we did not find any significant difference in the relative proportion of SIV-infected central memory and effector memory CD4⁺ T cells at either day 14 or day 42 p.i. (Supplemental Figure 2B). Overall, these data do not support the hypothesis that the absence of post-peak decline of viremia observed in CD4⁺ lymphocyte-depleted SIV-infected RMs is the result of an expanded in vivo cellular tropism of the virus for either monocytes or naive CD4⁺ T cells.

CD4⁺ lymphocyte-depleted SIV-infected RMs develop SIV-specific T cell responses similar to those of control animals. To determine whether CD4⁺ T cell depletion reduces the ability of SIV-infected RMs to generate virus-specific CD8⁺ T cell responses, we longitudinally compared the SIV-induced expansion of SIV-Gag- and SIV-Tat-specific CD8⁺ T cells within our experimental and control RMs, as assessed by staining with the Gag-CM9 or Tat-SL8 tetramers in the subset of Mamu-A*01 animals included in this study (3 CD4⁺ lymphocyte-depleted and 2 undepleted RMs). Despite some expected variation across individual RMs, we did not observe any consistent differences in the level of Gag- or Tat-specific CD8⁺ T cells between

the 2 groups of SIV-infected RMs in any of the tissues examined (Figure 5, A and B). To assess potential functional differences in the SIV-specific CD8⁺ T cell responses, we next assessed the ability of SIV-specific CD8⁺ T cells from both groups of RMs to produce the cytokines IFN- γ , IL-2, and TNF- α and/or to degranulate (as measured by surface expression of CD107a) in response to in vitro stimulation with peptides encompassing the entire SIV-Gag protein. These experiments did not reveal any consistent differences in the level or functionality of CD8⁺ T cells from CD4⁺ lymphocyte-depleted or control RMs at any of the examined time points (Figure 5C). Collectively, these data indicate that the marked depletion of CD4⁺ T cells induced by the Cdr-OKT4A-huIgG1 Ab did not compromise the generation of SIV-specific CD8⁺ T cell responses during primary SIV infection. Therefore, these data do not support the hypothesis that the absence of post-peak SIV replication decline observed in CD4⁺ lymphocyte-depleted RMs is a consequence of defective SIV-specific CD8⁺ T cell responses. Finally, we measured the level of SIV-specific CD4⁺ T cell responses using the same combination of in vitro stimulation with SIV peptides and intracellular cytokine staining (ICS; Figure 5D). The percentage of CD4⁺ T cells responding to SIV peptides was similar in the 2 groups. However, given the dramatically lower CD4⁺ T cell counts of the depleted animals (Figure 4A), these equivalent percentages resulted in much lower absolute numbers of SIV-specific CD4⁺ T cells/ μ l blood in experimental animals compared with controls (data not shown).

CD4⁺ lymphocyte-depleted RMs do not show differences in SIV-specific humoral responses during primary SIV infection. We next investigated whether the CD4⁺ lymphocyte-depleted SIV-infected RMs experienced defective and/or delayed SIV-specific humoral immune responses compared with control animals. To this end, we first measured the absolute count of total and activated (i.e., Ki67⁺) B cells in the blood and LNs during acute SIV infection and found no difference between CD4⁺ lymphocyte-depleted and control RMs (data not shown). We then measured the time to seroconversion for SIV-binding (i.e., non-neutralizing) Ab in the 2 groups of animals by standard ELISA and again found no significant difference (data not shown). Finally, we measured the ability of plasma isolated from CD4⁺ lymphocyte-depleted and control RMs at various time points after SIV infection to neutralize SIV_{mac251.6} infectivity in vitro. As shown in Figure 6, and as expected based on previous studies (25), the levels of neutralization were modest (i.e., reaching 50% inhibition only in RUv6) in both CD4⁺ lymphocyte-depleted and control SIV-infected RMs up to day 42 p.i. Although control animals showed slightly greater inhibition, no significant difference in neutralization was observed during acute or early chronic infection. Collectively, these data do not support the possibility that the difference in post-peak decline of viremia observed between CD4⁺ lymphocyte-depleted and control SIV-infected RMs was caused by a defective or delayed antiviral humoral immune response in CD4⁺ lymphocyte-depleted animals.

**Figure 5**

CD4⁺ lymphocyte-depleted SIV-infected RMs develop SIV-specific T cell responses similar to those of control animals. Longitudinal assessment of CD8⁺ T cell responses against 2 Mamu-A*01-restricted immunodominant epitopes of SIV-Gag (A) and Tat (B) in PBMCs, BM, and RB of a subset of Mamu-A*01⁺ RMs, as measured by tetramer staining. (C) SIV-specific CD8⁺ T cell responses after in vitro stimulation with SIV-Gag peptides, as measured in PBMCs by ICS, as well as expression of the degranulation marker CD107a by flow cytometry at days 11, 18, and 25 p.i. Horizontal lines denote medians. (D) SIV-specific CD4⁺ T cell responses after in vitro stimulation, as for CD8⁺ T cells.

CD4⁺ lymphocyte-depleted SIV-infected RMs show increased infection of non-T cells in LNs and RBs. The presence of high levels of virus replication in SIV-infected RMs with severe depletion of CD4⁺ T cells in all examined tissues prompted us to investigate the source of virus in these animals. To this end, we used a combined histological approach consisting of immunofluorescence or immunohistochemical (IHC) analysis for the pan-T cell marker CD3 and fluorescent in situ hybridization (ISH) for SIV in LN and RB sections from CD4⁺ lymphocyte-depleted and control animals. Figure 7, A and B, shows representative staining of LN and RB sections at day 28 p.i., with visual evidence of higher replication in non-T cells in the CD4⁺ lymphocyte-depleted RMs. As measured

by quantitative image analysis, SIV replication in CD3⁺ T cells versus CD3⁻ non-T cells in the LN showed a significant increase in percent virus harbored in CD3⁻ cells ($P = 0.0108$) in CD4⁺ lymphocyte-depleted RMs compared with control animals at day 28 p.i. Because of limited sample availability, we could not perform the same quantitative analysis in RB. However, the level of SIV replication in CD68⁺ macrophages and HLA-DM⁺ APCs in RBs appeared strikingly higher in CD4⁺ lymphocyte-depleted RMs (Figure 7D). Taken together, these results indicate that the CD4⁺ lymphocyte-depleting treatment was associated with a substantial increase in the level of virus replication in non-T cells such as macrophages and other APCs in tissues.

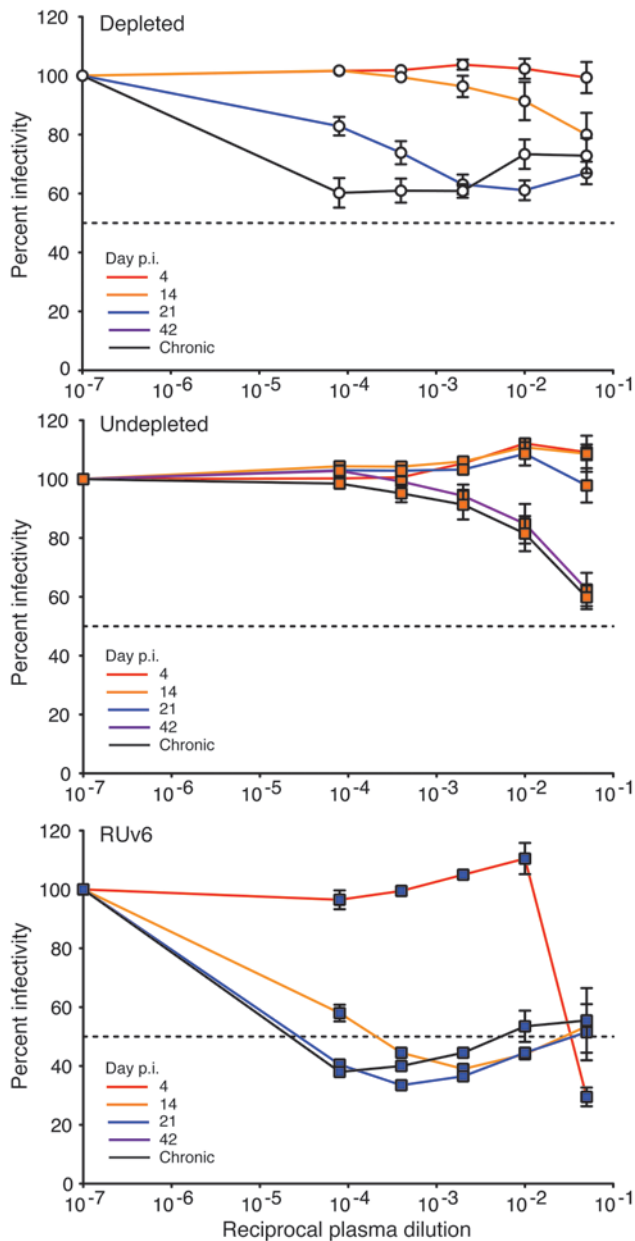


Figure 6

Low levels of plasma neutralizing activity against SIV in both CD4⁺ lymphocyte-depleted and control RMs. Percent infectivity of SIV_{mac251.6} in vitro after incubation with various dilutions of plasma collected at different time points p.i. in CD4⁺ lymphocyte-depleted and control RMs. RUv6, which experienced moderate CD4⁺ lymphocyte depletion, is also shown. Each line represents an individual time point. Dotted lines denote 50%. Individual points illustrate mean ± SEM per group or individual. Assay was performed twice independently with duplicate wells.

coreceptors in transfected 293T cells. As expected for SIV_{mac}, most Envs used CXCR6 and GPR15 efficiently and GPR1 to a lesser extent, but not CXCR4 or CCR2b. However, there was no increase in breadth or efficiency of alternative coreceptor use among Envs from CD4⁺ lymphocyte-depleted compared with undepleted RMs (data not shown). Thus, CD4⁺ lymphocyte depletion was associated with CD4-independent use of CCR5, but not with expanded alternative coreceptor utilization.

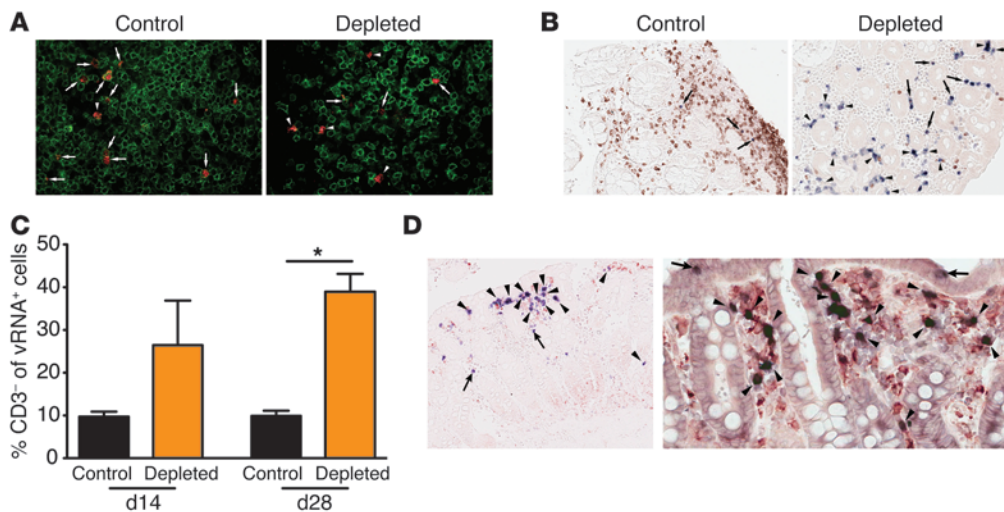
Discussion

CD4⁺ T cells play a central role in the immunopathogenesis of AIDS, and their attrition during chronic HIV infection is the main hallmark of disease progression. Importantly, CD4⁺ T cells may influence HIV and SIV replication in 2 contrasting ways, i.e., by acting as antiviral immune effector cells or by providing targets for virus replication (reviewed in refs. 2, 4–8). The antiviral role of CD4⁺ T cells could be further classified as direct (i.e., by the production of antiviral cytokines and cytotoxic activity) and indirect (i.e., as help to other immune effector cells, such as CD8⁺ T cells and B cells). In this study, we sought to dissect the in vivo role of CD4⁺ T cells as immune effectors and targets for virus replication by depleting these cells prior to SIV infection of RMs. We chose an experimental system in which CD4⁺ T cells are depleted from blood, LNs, and BM, but not mucosal effector sites. This methodology allowed for the preservation of sufficient (and canonical) targets for early virus replication, avoiding the possibility of abortive infection, while eliminating or at least dramatically reducing a primary CD4⁺ T cell response.

We considered 2 alternative outcomes for the kinetics of virus replication during acute SIV infection in CD4⁺ lymphocyte-depleted RMs: (a) an increased peak and/or reduced post-peak decline of viremia, which would indicate that the primary effect of removing CD4⁺ T cells is the loss of an important immune effector function; or (b) a decreased peak and/or a more rapid post-peak decline, which would indicate that the primary effect of removing CD4⁺ T cells is a reduction of target cells for virus replication. The results of this study clearly showed a normal peak of viremia but the absence of a post-peak viral decline in the CD4⁺ lymphocyte-depleted SIV-infected RMs, supporting the hypothesis that CD4⁺ T cells are essential to establish control of virus replication during acute SIV infection. To the best of our knowledge, this is the first time that this conclusion has been reached through a direct experimental approach. Importantly, CD4⁺ lymphocyte-depleted SIV-infected RMs also showed accelerated disease progression compared with control animals. This phenomenon may be attributed to higher setpoint viremia, lower CD4⁺ T cell counts, or both, and the current experimental setting did not allow us to discriminate between these 2 possibilities.

To examine the pathophysiologic mechanisms by which depletion of CD4⁺ T cells results in abrogation of the post-peak decline of viremia, we first considered the possibility that the

Virus from CD4⁺ lymphocyte-depleted SIV-infected RMs develops CD4-independent envelopes. Finally, to determine whether CD4⁺ lymphocyte depletion was associated with changes in viral envelope (Env) receptor/coreceptor utilization patterns, we generated a panel of envs by single genome amplification (SGA) from plasma of 7 RMs (5 depleted and 2 undepleted) at day 42 p.i. and analyzed infection patterns using pseudotype reporter viruses. As shown in Figure 8, none of the Envs from the undepleted animals used CCR5 independently of CD4. In contrast, Envs from 4 of the 5 depleted RMs were able to infect CCR5⁺ cells in the absence of CD4 at levels approximating 40%–60% of those seen in CCR5⁺CD4⁺ cells. Lower, but nonetheless detectable, levels of CD4-independent infection were seen with Envs from RUv6, the animal that exhibited only moderate CD4⁺ T cell depletion. Concordant results were seen when CCR5⁺CD4⁺ U87 cells were treated with a CD4-blocking mAb (data not shown). We also examined use of alternative

**Figure 7**

CD4⁺ lymphocyte-depleted SIV-infected RMs show increased infection of non-T cells in LNs and RBs. Representative images of LN sections (A), using SIV fluorescence ISH with CD3 immunofluorescence, and RB sections (B), using chromogenic SIV ISH with CD3 IHC, from untreated control and CD4⁺ lymphocyte-depleted RMs at day 28 p.i. Arrows denote CD3⁺SIV vRNA⁺ cells; arrowheads denote CD3⁺SIV vRNA⁺ cells. (C) Percent CD3⁺SIV vRNA⁺ cells from LN sections of control and CD4⁺ lymphocyte-depleted RMs at days 14 and 28 p.i. *P = 0.0108, Student's t test. (D) Representative images from RB sections using chromogenic SIV ISH with HLA-DM (left) and CD68 (right) IHC from CD4⁺ lymphocyte-depleted animals. Arrowheads, HLA-DM⁺ or CD68⁺SIV vRNA⁺ cells; arrows, HLA-DM⁻ or CD68⁻SIV vRNA⁺ cells. Original magnification, $\times 600$ (A); $\times 200$ (B and D, left); $\times 400$ (D, right).

CD4⁺ lymphocyte-depleting treatment was followed by a paradoxical increase in the number of CD4⁺ target cells for SIV replication. It was conceivable that, although we used a CD4⁺ lymphocyte-depleting Ab, the treated RMs may have had increased numbers of activated and/or proliferating CD4⁺ T cells as a result of strong stimulation by homeostasis-driven CD4⁺ T cell tropic cytokines such as IL-7 and IL-15 (30). We therefore measured the absolute numbers of proliferating and/or CCR5⁺ total and memory CD4⁺ T cells that could serve as preferential targets for SIV infection in blood, LNs, and mucosal tissues. This analysis did not reveal any sign of an increased number of CD4⁺ target cells in CD4⁺ lymphocyte-depleted SIV-infected RMs, except for a modest increase in the fraction of activated/CCR5⁺CD4⁺ T cells in the RB at a p.i. time at which the vast majority of mucosal CD4⁺ T cells had been depleted, in agreement with numerous previous studies (17, 18, 31, 32). In addition, we found no evidence of an expanded cell tropism of SIV for either naive CD4⁺ T cells or circulating monocytes as a possible contributor to the higher viremia in the CD4⁺ lymphocyte-depleted SIV-infected RMs. The current set of data does not exclude the possibility that higher levels of activated and/or infected CD4⁺ T cells are present in anatomic compartments that were not examined as part of this study, nor that SIV replication was higher on a per-cell basis in CD4⁺ lymphocyte-depleted RMs. These caveats notwithstanding, we conclude that the bulk of the available experimental data are not consistent with the idea that CD4⁺ lymphocyte depletion results in a paradoxical increase in CD4⁺ target cells.

We next sought to determine whether the loss of an antiviral effect of CD4⁺ T cells in CD4⁺ lymphocyte-depleted SIV-infected RMs was due to reduced effectiveness of CD8⁺ T cells and/or Ab-producing B cells. We measured SIV-specific cellular immune

responses by both ICS and tetramer staining as well as humoral responses by assessment of B cell activation and production of both SIV binding and neutralizing Abs. This analysis did not reveal any obvious defect of SIV-specific CD8⁺ T cell-mediated responses in the CD4⁺ lymphocyte-depleted RMs during the first 42 days of infection that could explain the lack of post-peak decline of viremia in these animals. This result was actually not surprising, as primary virus-specific CD8⁺ T cell responses have previously been shown to be by and large CD4⁺ T cell independent in numerous experimental models (20–22). In addition, we did not detect any difference in SIV-specific B cell responses in CD4⁺ lymphocyte-depleted RMs compared with controls. One explanation for

this finding is that the residual CD4⁺ T cells present in depleted SIV-infected RMs may have been sufficient to provide the required help for SIV-specific B cells. It should also be noted that the induction of potent anti-SIV neutralizing Ab responses is reported to occur several weeks, if not months, after infection (23–25, 33). This time frame is not consistent with a major role for these Abs in the post-peak decline of viremia that occurs between day 14 and 21 p.i. Collectively, these data are consistent with the hypothesis that the abrogation of direct CD4⁺ T cell-mediated antiviral immune responses is the main determinant of the lack of post-peak decline of viremia in CD4⁺ lymphocyte-depleted SIV-infected RMs. It should be noted, however, that in this study we did not assess directly the cytolytic activity of SIV-specific CD4⁺ T cells in either group of animals, nor did we analyze the ability of CD8⁺ T cells to directly inhibit virus replication. Moreover, the presented data do not rule out that non-neutralizing Abs and/or ADCC activity play a role in the early control of virus replication that could be reduced in the absence of CD4 help. Therefore, we cannot exclude the possibility that subtle differences in the in vivo antiviral function of CD8⁺ T cells or in the SIV-specific Ab function between CD4⁺ lymphocyte-depleted and control RMs are involved in the observed phenotype.

Several previous studies have provided evidence in support of a direct antiviral role of CD4⁺ T cells during both HIV and SIV infection (34–42). However, this antiviral effect has not been formally tested in vivo by depleting CD4⁺ T cells in SIV-infected RMs (analogous to the classical experiments of CD8⁺ lymphocyte depletion). The current study provides the first direct experimental evidence to our knowledge that CD4⁺ T cells are necessary to achieve a post-peak decline of SIV viremia in RMs. In addition to the well-known helper effect, HIV- and

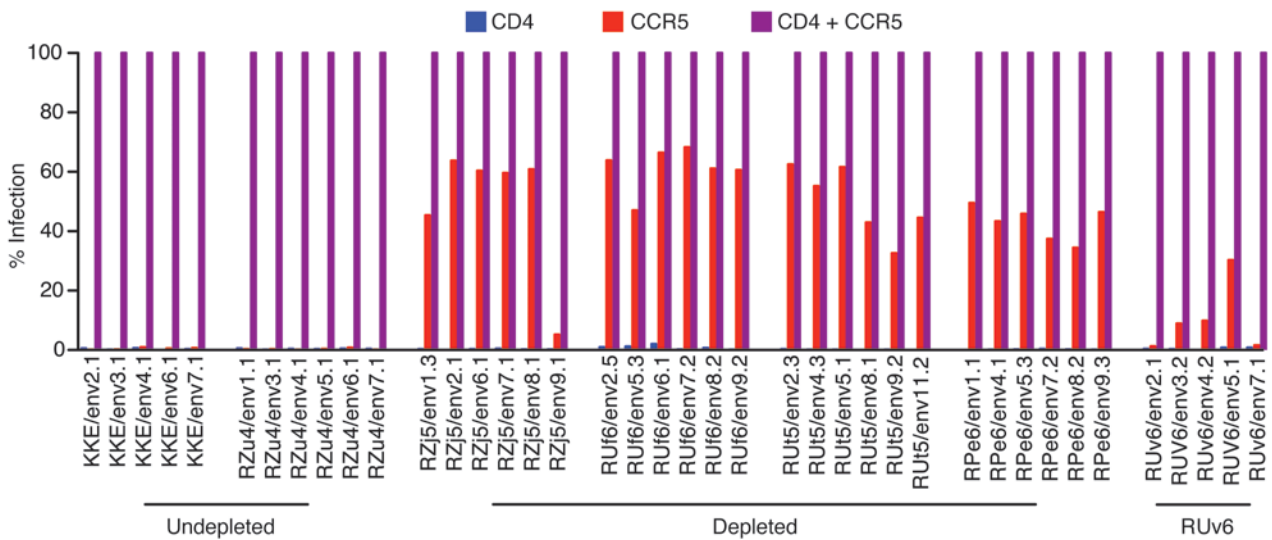


Figure 8

Emergence of CD4-independent SIV envelopes in CD4-depleted, but not undepleted, RMs. Env clones were obtained by SGA from plasma at day 42 p.i. and used to generate luciferase-expressing pseudotype reporter viruses. Pseudotype virus was used for infection of 293T cells transfected with CD4 alone, CCR5 alone, or CD4 and CCR5 together. Infection based on luciferase activity in cell lysates was normalized relative to that mediated by CCR5 and CD4 together for each Env.

SIV-specific CD4+ T cells may directly inhibit virus replication through granzyme B and/or perforin-mediated cytolytic activity and through production of antiviral cytokines and chemokines (36–38, 41–43).

The presence of very high virus replication in the context of the severe, generalized CD4+ T cell depletion observed in the anti-CD4 Ab treated RMs prompted us to investigate the cellular origin and coreceptor use of the virus in these animals. These experiments revealed that CD4+ lymphocyte depletion induced a significant increase in the level of virus replication occurring in non-T cells, such as tissue macrophages and other APCs, which was coupled to the emergence of CD4-independent virus strains. Possible explanations for this change in the pattern of in vivo SIV-infected cells may be related to a lack of canonical CD4+ T cell targets (44, 45) and/or the absence of an antiviral effect mediated by CD4+ T cells (or other immune effector functions). While the current set of data cannot distinguish between these 2 possibilities, further studies aimed at better understanding the relationship between CD4+ T cell loss and virus replication in non-T cells during SIV infection of RMs are warranted.

The results of this work have particular relevance both for the understanding of AIDS immunopathogenesis and for HIV vaccine design. Currently, much emphasis is placed on candidate AIDS vaccines that would protect from HIV transmission and/or disease progression by eliciting neutralizing Abs and CD8+ CTLs (1). The current study suggests that, in addition to humoral and/or CD8+ T cell-mediated immune responses, the antiviral CD4+ T cell response may play an important role in limiting HIV replication, a finding that could be exploited in the design of candidate AIDS vaccines. As CD4+ T cell activation induced by an AIDS vaccine has the intrinsic potential of generating more targets for HIV (and SIV) infection (46), it will be essential to investigate at the phenotypic and functional level what type of CD4+ T cell responses mediate the protective antiviral effect revealed in this study.

Methods

Animals and virus. Of the 9 healthy, SIV-uninfected Indian RMs (Macaca mulatta) used in this study, 5 were Mamu-A*01+ and 4 were Mamu-A*01-. These animals were housed at the Yerkes National Primate Research Center and maintained in accordance with NIH guidelines. All animals were infected i.v. with 3,000 TCID50 SIVmac251 (provided by C. Miller, UCD, Davis, California, USA). Animals that reached disease endpoint, as defined by wasting syndrome unresponsive to therapy, were sacrificed according to the recommendations of the 2007 American Veterinary Medical Association (AVMA) Guidelines on Euthanasia.

CD4+ lymphocyte depletion. 5 uninfected RMs (3 Mamu-A*01+, 2 Mamu-A*01-) were treated i.v. with 10 mg/kg humanized anti-CD4 mAb (Cdr-OKT4A-huIgG1; clone 12F11; provided by K. Reimann, Beth Israel Deaconess Medical Center, Boston, Massachusetts, USA) at days -57, -52, -47, and -45 relative to SIV infection. The efficacy of the depleting treatment in tissues in which absolute number calculations of the total lymphoid cellularity were not performed was assessed assuming that the non-CD4+ T cell fraction remained unchanged after the anti-CD4 Ab treatment.

Determination of viral load RNA. Quantitative real-time RT-PCR assay to determine SIV viral load was performed as previously described (47).

Tissue collection and sample processing. PBMCs were stained in whole blood and lysed with 1x BD FACS Lysing Solution prior to intracellular staining. Procedures for LN biopsy and RB as well as for isolation of lymphocytes from these samples were performed as previously described (48). All samples were processed, fixed (1% paraformaldehyde), and analyzed within 24 hours of collection.

Flow cytometry and immunophenotyping. Polychromatic flow cytometry analysis was performed on an LSR II equipped with FACS DiVA software (version 6.1.1; BD). The following Abs were used at predetermined volumes: CCR5-PE (clone 3A9), CCR7-PECy7 (clone 3D12), CD3-Alexa Fluor 700 (clone SP34-2), CD8-APCCy7 (clone SK1), CD14-PE (clone MSE2), CD107a-FITC (clone H4A3), IFN-gamma-PE (clone B27), IL-2-APC (clone MQ1-17H12), Ki67-FITC (clone B56), and TNF-alpha-PECy7 (clone MAB11) from BD Biosciences - Pharmingen; CD4-Pacific Blue (clone OKT4) and CD95-PECy5 (clone DX2) from eBiosciences; CD20-ECD (clone B9E9) and



CD28-ECD (clone 28.2) from Beckman-Coulter. MHC class I tetramers specific for SIV-immunodominant epitopes Gag₁₈₁₋₁₈₉ CM9 (CTPYDINQM) and Tat₂₈₋₃₅ SL8 (STPESANL) were prepared as previously described (49) and conjugated to streptavidin-allophycocyanin fluorophore (Invitrogen). Cells were permeabilized with 1× BD FACS Permeabilizing Solution 2 prior to intracellular staining with Ki67. The data acquired were analyzed using FlowJo software (version 8.8.4; TreeStar). For all analyses, we used a threshold cutoff of 100 collected events.

Determination of antigen-specific CD8⁺ T cell responses. SIV-specific CD8⁺ T cell responses were measured by flow cytometry using ICS in response to pools of 15-mer peptides overlapping by 11 amino acids and spanning the entire sequence of the SIV_{mac239} Gag, as previously described (50). Complete peptide sets for SIV_{mac239} were obtained from the NIH AIDS Research and Reference Reagent Program.

Neutralization assay. Plasma samples from experimental animals were tested for neutralizing Ab activity by the ability to neutralize SIV_{mac251.6}, as previously described (51, 52). Briefly, Env-pseudotyped virions were incubated with serial dilutions of heat-inactivated plasma and added to JCS5BL-13 (Tzm-bl) cells. Cells were incubated for 2 days and then lysed, and the luciferase activity for each well was assessed. Percent infectivity was calculated by dividing luciferase units from wells at each plasma dilution by values obtained from control (no plasma) wells. Each experiment was performed twice independently with duplicate wells.

Quantitative PCR for SIV gag DNA. Sorting of CD4⁺ T cell subsets was performed on a FACS Aria III Cell Sorter (BD). Cells were initially gated based on characteristic light scatter properties. Live CD3⁺CD4⁺ T cells were characterized as either naive (CD28⁺CD95⁺CCR7⁺), central memory (CD28⁺CD95^{lo}CCR7⁺), or effector memory (CD28⁻CD95^{lo}CCR7⁻). Live monocytes were defined as CD14⁺CD4^{lo}. Quantification of SIV_{mac} gag DNA was performed by quantitative PCR by the 5' nuclease (TaqMan) assay with an ABI7700 system (PerkinElmer Life and Analytical Sciences), as previously described (53). For cell number quantification, quantitative PCR was performed simultaneously for monkey albumin gene copy number. The sequence of the forward primer for SIV_{mac} was 5'-GTCTGCGTCAT(T/C)TGGTGCATTC-3'; the reverse primer sequence was 5'-CACTAG(C/T)TGTCTCTGCACTAT(A/G)TGTTTTG-3'.

SIV fluorescent ISH, double ISH/IHC, and quantitative image analysis. We designed and developed highly sensitive digoxigenin-labeled SIV_{mac239} riboprobes for ISH. These newly designed SIV riboprobes were generated by PCR-based cloning of target regions in gag, pol, vif/vpx/vpr, env, and rev (9 riboprobes) of roughly equal size (~600 bp), allowing for equal stoichiometric molar equivalent riboprobes in our riboprobe cocktail. SIV fluorescence ISH and double ISH/IHC was modified from previously published ISH procedures (54). In brief, 5-mm tissue sections were mounted on Superfrost Plus Microscope Slides (Fisher Scientific), dewaxed, and rehydrated in double-distilled H₂O. Slides were immersed at room temperature (RT) in 0.2 N HCl for 30 minutes, 0.15 M triethanolamine (pH 7.4) for 15 minutes, and 0.005% digitonin for 5 minutes. The slides were then incubated for 30 minutes at 37°C in a Tris-buffered solution containing 2 mM CaCl₂ and proteinase K (5 mg/ml). Alternatively, for ISH combined with HLA-DM (Sigma-Aldrich) or CD68 (clone KP1; Dako) IHC, after rehydrating in double-distilled H₂O, the slides were treated with heat-induced epitope retrieval (HIER) in lieu of proteinase K digestion using 1× Diva buffer (Biocare Medical) in a pressure cooker (122°C, 30 seconds; Biocare Medical deocloaking chamber). After either HIER or proteinase K digestion, slides were washed in HyPure molecular biology-grade H₂O (Hyclone; Thermo Scientific), acetylated (0.25% acetic anhydride) for 20 minutes, and placed in 0.1 M triethanolamine (pH 8.0) until hybridization. Sections were then covered with hybridization solution (50% deionized formamide, 10% dextran sulfate, 0.6 M NaCl, 0.4 mg/ml yeast RNA [Ambion Inc.], and

1× Denhardt medium in 20 mM HEPES buffer [pH 7.2] with 1 mM EDTA) containing 100–400 ng/ml pooled SIV riboprobes and hybridized for 18 hours at 48°C. After hybridization, slides were washed in 5× SSC (1× SSC = 0.15 M NaCl + 0.015 M Sodium Citrate) at 42°C for 20 minutes, 2× SSC in 50% formamide at 50°C for 20 minutes, and 1× RWS buffer at 37°C with ribonuclease A (25 µg/ml) and T1 (25 U/ml) for 30 minutes. After washing in RWS buffer, 2× SSC, and 0.1× SSC at 37°C for 15 minutes each, sections were transferred to 1× Tris-buffered saline (TBS; Boston BioProducts) containing 0.05% Tween-20 (TBS-Tw). Tissues were blocked in TBS containing either 2% sheep serum (double ISH/IHC) or 2% donkey serum (fluorescence ISH) for 1 hour at RT and incubated with either sheep Fab anti-digoxigenin (Roche Applied Science) at 1:500 in TBS containing 2% sheep serum (double ISH/IHC) or mouse anti-digoxigenin (Jackson ImmunoResearch) at 1:2,000 in TBS containing 2% donkey serum (for fluorescence ISH) with rabbit monoclonal anti-CD3 (clone SP7; Labvision) for 1 hour at RT or overnight at 4°C. For double SIV ISH/IHC, tissues were washed in TBS-Tw, incubated with Polink-1 Rabbit HRP 1-step polymer system (Golden Bridge International Labs) for 30 minutes, developed with ImmPact NovaRED peroxidase substrate (Vector Laboratories) for 2–10 minutes, washed in TBS-Tw, incubated with the alkaline phosphatase substrate NBT/BCIP containing levamisole (Roche Applied Science) for 2–6 hours, placed into double-distilled H₂O, covered in Clear-Mount (Electron Microscopy Systems), dried, cleared in xylenes, and coverslipped with Permount (Fisher). Double ISH/IHC slides were scanned at high magnification (×400) using the ScanScope CS System (Aperio Technologies Inc.). Representative high-magnification (×200 or ×400) images were acquired from these whole tissue scans. For SIV fluorescence ISH, slides were washed in TBS-Tw, incubated with goat anti-mouse DyLight-594 (Jackson ImmunoResearch) for 1 hour at RT, washed in TBS-Tw, incubated with donkey anti-rabbit-Alexa Fluor 488 (Invitrogen) and donkey anti-goat-Alexa Fluor 594 (Invitrogen) containing 300 nM DAPI for 1 hour at RT, washed in TBS-Tween, mounted in Aqua-Poly mount (Polysciences Inc.), and imaged using a Nikon 80i fluorescent microscope with a metal halide illuminator. 8–10 high-magnification (×600) monochromatic images were randomly acquired from the T cell zone, images were merged in Photoshop CS3 (Adobe), the number of SIV viral RNA-positive (vRNA⁺) cells that were CD3⁺ and CD3⁻ was manually counted per high-powered field, and the proportions were determined.

Analysis of viral envelopes. Complete viral env genes (plus rev) were PCR-amplified from plasma obtained at day 42 p.i. using a procedure for endpoint diluted single genomes (51, 52, 55). Briefly, vRNA was purified from plasma using the QIAamp Viral RNA purification kit (Qiagen), and cDNA was prepared using Superscript III (Invitrogen) and the primer SM-ER1 (see below). First-round PCR amplification was performed on endpoint diluted cDNA using forward primer H2SM-EF1 (5'-CCCTGAAGGMGCMRGAGAGCTCATT-3') and reverse primer SM-ER1 (5'-CTATCACTGTAATAAATCCCTCCAGTCCC-3'). Second-round PCR amplification was performed using forward primer H2SM-EF2 (5'-CACCTAAAARTGYTGCTAYCATTGCCAG-3'; modified for directional cloning) and reverse primer SM-ER2 (5'-ATAAATGAGACATGCTATTGCCAATTTG-3'). PCR amplicons were cloned into the pCDNA3.1V5HisTOPO-TA plasmid expression vector, and transformed colonies that contained an insert were identified through a PCR screen. Env-containing plasmids were recovered and used to generate pseudotyped virions, and coreceptor-mediated target cell infection was analyzed as previously described (56). Briefly, 293T cells were cotransfected with env expression plasmids and the HIV-1 luciferase-expressing env-deleted pNL-luc-E-R+ vector. Pseudotypes were harvested 2 days later and quantified by infection of U87/CD4/CCR5 cells. Equal amounts of each pseudotype (10⁵ RLU as measured in U87/CD4/CCR5 cells) were then used



to infect 293T cells transfected with CD4 alone, CCR5 alone, or both together. Cells were lysed 3 days later, and infection was measured by luciferase activity in cell lysates.

Statistics. Statistical analyses were performed using Prism (version 4.0; GraphPad Software Inc.) or SAS 9.1 (SAS Institute Inc.). 1-tailed Student's *t* tests were performed to determine the significance of changes in the percent or count of CD4⁺CD3⁺ T cells relative to baseline (paired) or in the difference of particular cell subsets at single time points in or among CD4⁺ lymphocyte-depleted and control animals (unpaired). Welch corrections were applied as indicated. The Mann-Whitney test was performed on samples that received stimulation or were sorted for PCR. A mixed linear-effects model was used to assess the longitudinal significance of differences in the percent and count of peripheral CD3⁺CD4⁺ T cells between groups as well as setpoint viral load. Pearson correlation was performed between the absolute number of CD3⁺CD4⁺ T cells and the percentage of circulating Ki67⁺CD4⁺ T cells. The Kaplan-Meier estimate was applied to survival data to determine survival significance between CD4⁺ lymphocyte-depleted and control animals. Averaged data are presented as arithmetic mean ± SEM. A *P* value less than 0.05 was considered significant.

Study approval. Animal studies were conducted in accordance with protocols approved by the IACUCs of University of Pennsylvania and Emory University.

Acknowledgments

We acknowledge Stephanie Ehnert, Chris Souder, and all the animal care and veterinary staff at the Yerkes National Primate

Research Center; the Virology Core of the Emory Center for AIDS Research (CFAR); the University of Pennsylvania CFAR; the University of Pennsylvania Flow Cytometry Core; and the NIH nonhuman primate reagent resource. We also thank Ann Chahroudi for critical reading of this manuscript. The Cdr-OKT4A-huIgG1 depleting mAb used in this study was provided by Keith Reimann. The SIV_{mac251} used to infect the RMs was provided by Chris Miller. This work was supported by NIH grants AI-66998 (to G. Silvestri) and RR-00165 (to Yerkes National Primate Research Center). This project has been funded in part with federal funds from the National Cancer Institute, NIH, under Contract No. HHSN261200800001E. The content of this publication does not necessarily reflect the views or policies of the Department of Health and Human Services, nor does mention of trade names, commercial products, or organizations imply endorsement by the U.S. government.

Received for publication December 6, 2010, and accepted in revised form September 7, 2011.

Address correspondence to: Guido Silvestri, Yerkes National Primate Research Center and Emory University School of Medicine, 3014 EVC Building, 954 Gatewood Road NE, Atlanta, Georgia 30033, USA. Phone: 404.727.9139; Fax: 404.727.9139; E-mail: gsilves@emory.edu.

- Mcmichael AJ, Borrow P, Tomaras GD, Goonetilleke N, Haynes BF. The immune response during acute HIV-1 infection: clues for vaccine development. *Nat Rev Immunol.* 2010;10(1):11-23.
- Haase AT. Targeting early infection to prevent HIV-1 mucosal transmission. *Nature.* 2010; 464(7286):217-223.
- Wu L, Kewal Ramani VN. Dendritic-cell interactions with HIV: infection and viral dissemination. *Nat Rev Immunol.* 2006;6(11):859-868.
- Picker LJ, Maino VC. The CD4(+) T cell response to HIV-1. *Curr Opin Immunol.* 2000;12(4):381-386.
- Norris PJ, Rosenberg ES. CD4(+) T helper cells and the role they play in viral control. *J Mol Med.* 2002; 80(7):397-405.
- Phillips AN. Reduction of HIV concentration during acute infection: independence from a specific immune response. *Science.* 1996;271(5248):497-499.
- Kelleher AD, Zaunders JJ. Decimated or missing in action: CD4+ T cells as targets and effectors in the pathogenesis of primary HIV infection. *Curr HIV/AIDS Rep.* 2006;3(1):5-12.
- Picker LJ. Immunopathogenesis of acute AIDS virus infection. *Curr Opin Immunol.* 2006;18(4):399-405.
- Schmitz JE, et al. Control of viremia in simian immunodeficiency virus infection by CD8+ lymphocytes. *Science.* 1999;283(5403):857-860.
- Jin X, et al. Dramatic rise in plasma viremia after CD8(+) T cell depletion in simian immunodeficiency virus-infected macaques. *J Exp Med.* 1999; 189(6):991-998.
- Matano T, Shibata R, Siemon C, Connors M, Lane HC, Martin MA. Administration of an anti-CD8 monoclonal antibody interferes with the clearance of chimeric simian/human immunodeficiency virus during primary infections of rhesus macaques. *J Virol.* 1998;72(1):164-169.
- Mascola JR, et al. Protection of macaques against vaginal transmission of a pathogenic HIV-1/SIV chimeric virus by passive infusion of neutralizing antibodies. *Nat Med.* 2000;6(2):207-210.
- Baba TW, et al. Human neutralizing monoclonal antibodies of the IgG1 subtype protect against mucosal simian-human immunodeficiency virus infection. *Nat Med.* 2000;6(2):200-206.
- Hessell AJ, et al. Fc receptor but not complement binding is important in antibody protection against HIV. *Nature.* 2007;449(7158):101-104.
- Ng CT, et al. Passive neutralizing antibody controls SHIV viremia and enhances B cell responses in infant macaques. *Nat Med.* 2010;16(10):1117-1119.
- Garber DA, et al. Blockade of T cell costimulation reveals interrelated actions of CD4+ and CD8+ T cells in control of SIV replication. *J Clin Invest.* 2004; 113(6):836-845.
- Veazey RS, et al. Gastrointestinal tract as a major site of CD4+ T cell depletion and viral replication in SIV infection. *Science.* 1998;280(5362):427-431.
- Mattapallil JJ, Douek DC, Hill B, Nishimura Y, Martin M, Roederer M. Massive infection and loss of memory CD4+ T cells in multiple tissues during acute SIV infection. *Nature.* 2005;434(7037):1093-1097.
- Miller CJ, et al. Propagation and dissemination of infection after vaginal transmission of simian immunodeficiency virus. *J Virol.* 2005;79(14):9217-9227.
- Shedlock DJ, Shen H. Requirement for CD4 T cell help in generating functional CD8 T cell memory. *Science.* 2003;300(5617):337-339.
- Sun JC, Bevan MJ. Defective CD8 T cell memory following acute infection without CD4 T cell help. *Science.* 2003;300(5617):339-342.
- Sun JC, Williams MA, Bevan MJ. CD4+ T cells are required for the maintenance, not programming, of memory CD8+ T cells after acute infection. *Nat Immunol.* 2004;5(9):927-933.
- Cole KS, et al. Evolution of envelope-specific antibody responses in monkeys experimentally infected or immunized with simian immunodeficiency virus and its association with the development of protective immunity. *J Virol.* 1997;71(7):5069-5079.
- Connor RI, et al. Immunological and virological analyses of persons infected by human immunodeficiency virus type 1 while participating in trials of recombinant gp120 subunit vaccines. *J Virol.* 1998; 72(2):1552-1576.
- Yeh WW, et al. Autologous neutralizing antibodies to the transmitted/founder viruses emerge late after simian immunodeficiency virus SIVmac251 infection of rhesus monkeys. *J Virol.* 2010;84(12):6018-6032.
- Reimann KA, et al. A humanized form of a CD4-specific monoclonal antibody exhibits decreased antigenicity and prolonged plasma half-life in rhesus monkeys while retaining its unique biological and antiviral properties. *AIDS Res Hum Retroviruses.* 1997;13(11):933-943.
- Klatt NR, et al. Availability of activated CD4+ T cells dictates the level of viremia in naturally SIV-infected sooty mangabeys. *J Clin Invest.* 2008; 118(6):2039-2049.
- Ingram JC, et al. Lineage-specific T-cell reconstitution following in vivo CD4+ and CD8+ lymphocyte depletion in nonhuman primates. *Blood.* 2010;116(5):748-758.
- Paiardini M, et al. Bone marrow-based homeostatic proliferation of mature T cells in nonhuman primates: implications for AIDS pathogenesis. *Blood.* 2009;113(3):612-621.
- Surh CD, Sprent J. Homeostasis of naive and memory T cells. *Immunity.* 2008;29(6):848-862.
- Pandrea IV, et al. Acute loss of intestinal CD4+ T cells is not predictive of simian immunodeficiency virus viremia. *J Immunol.* 2007;179(5):3035-3046.
- Gordon SN, et al. Severe depletion of mucosal CD4+ T cells in AIDS-free simian immunodeficiency virus-infected sooty mangabeys. *J Immunol.* 2007;179(5):3026-3034.
- Fultz PN, Stricker RB, McClure HM, Anderson DC, Switzer WM, Horaist C. Humoral response to SIV/SMM infection in macaque and mangabey monkeys. *J Acquir Immune Defic Syndr.* 1990;3(4):319-329.
- Rosenberg ES, et al. Vigorous HIV-1-specific CD4+ T cell responses associated with control of viremia. *Science.* 1997;278(5342):1447-1450.
- Pitcher CJ, et al. HIV-1-specific CD4+ T cells are detectable in most individuals with active HIV-1 infection, but decline with prolonged viral suppression. *Nat Med.* 1999;5(5):518-525.
- Norris PJ, et al. Multiple effector functions mediated by human immunodeficiency virus-specific CD4(+) T-cell clones. *J Virol.* 2001;75(20):9771-9779.
- Appay V, et al. Characterization of CD4(+) CTLs ex vivo. *J Immunol.* 2002;168(11):5954-5958.



38. Norris PJ, et al. Beyond help: direct effector functions of human immunodeficiency virus type 1-specific CD4(+) T cells. *J Virol*. 2004;78(16):8844–8851.
39. Seth N, Kaufmann D, Lahey T, Rosenberg ES, Wucherpfennig KW. Expansion and contraction of HIV-specific CD4 T cells with short bursts of viremia, but physical loss of the majority of these cells with sustained viral replication. *J Immunol*. 2005; 175(10):6948–6958.
40. Scriba TJ, et al. HIV-1-specific CD4+ T lymphocyte turnover and activation increase upon viral rebound. *J Clin Invest*. 2005;115(2):443–450.
41. Sacha JB, et al. Gag- and Nef-specific CD4+ T cells recognize and inhibit SIV replication in infected macrophages early after infection. *Proc Natl Acad Sci U S A*. 2009;106(24):9791–9796.
42. Zheng N, Fujiwara M, Ueno T, Oka S, Takiguchi M. Strong ability of Nef-specific CD4+ cytotoxic T cells to suppress human immunodeficiency virus type 1 (HIV-1) replication in HIV-1-infected CD4+ T cells and macrophages. *J Virol*. 2009;83(15):7668–7677.
43. Hahn S, Erb P. The immunomodulatory role of CD4-positive cytotoxic T-lymphocytes in health and disease. *Int Rev Immunol*. 1999;18(5–6):449–464.
44. Igarashi T, et al. Macrophage are the principal reservoir and sustain high virus loads in rhesus macaques after the depletion of CD4+ T cells by a highly pathogenic simian immunodeficiency virus/HIV type 1 chimera (SHIV): Implications for HIV-1 infections of humans. *Proc Natl Acad Sci U S A*. 2001; 98(2):658–663.
45. Brown CR, et al. Unique pathology in simian immunodeficiency virus-infected rapid progressor macaques is consistent with a pathogenesis distinct from that of classical AIDS. *J Virol*. 2007; 81(11):5594–5606.
46. Benlahrech A, et al. Adenovirus vector vaccination induces expansion of memory CD4 T cells with a mucosal homing phenotype that are readily susceptible to HIV-1. *Proc Natl Acad Sci U S A*. 2009; 106(47):19940–19945.
47. Amara RR, et al. Control of a mucosal challenge and prevention of AIDS by a multiprotein DNA/MVA vaccine. *Science*. 2001;292(5514):69–74.
48. Sumpter B, et al. Correlates of preserved CD4(+) T cell homeostasis during natural, nonpathogenic simian immunodeficiency virus infection of sooty mangabeys: implications for AIDS pathogenesis. *J Immunol*. 2007;178(3):1680–1691.
49. Altman JD, et al. Phenotypic analysis of antigen-specific T lymphocytes. *Science*. 1996;274(5284):94–96.
50. Dunham R, et al. The AIDS resistance of naturally SIV-infected sooty mangabeys is independent of cellular immunity to the virus. *Blood*. 2006; 108(1):209–217.
51. Li B, et al. Evidence for potent autologous neutralizing antibody titers and compact envelopes in early infection with subtype C human immunodeficiency virus type 1. *J Virol*. 2006;80(11):5211–5218.
52. Li B, et al. Nonpathogenic simian immunodeficiency virus infection of sooty mangabeys is not associated with high levels of autologous neutralizing antibodies. *J Virol*. 2010;84(12):6248–6253.
53. Okoye A, et al. Progressive CD4+ central memory T cell decline results in CD4+ effector memory insufficiency and overt disease in chronic SIV infection. *J Exp Med*. 2007;204(9):2171–2185.
54. Haase AT, et al. Quantitative image analysis of HIV-1 infection in lymphoid tissue. *Science*. 1996; 274(5289):985–989.
55. Haaland RE, et al. Inflammatory genital infections mitigate a severe genetic bottleneck in heterosexual transmission of subtype A and C HIV-1. *PLoS Pathog*. 2009;5(1):e1000274.
56. Riddick NE, et al. A novel CCR5 mutation common in sooty mangabeys reveals SIVsmm infection of CCR5-null natural hosts and efficient alternative coreceptor use in vivo. *PLoS Pathog*. 2010;6(8):e1001064.